Passivity-Based Control Applied of a Reaction Wheel Pendulum: an IDA-PBC Approach

Oscar Danilo Montoya, Víctor Manuel Garrido,
Walter Gil-González and Cesar Orozco-Henao

December 4, 2019

Passivity-Based Control Applied of a Reaction Wheel Pendulum: an IDA-PBC Approach

Oscar Danilo Montoya and Víctor Manuel Garrido
Programa de Ingeniería Eléctrica
Universidad Tecnológica de Bolívar
Cartagena, Colombia
E-mail: {omontoya,vgarrido}@utb.edu.co

Walter Gil-González
Programa de Ingeniería Eléctrica
Universidad Tecnológica de Pereira
Pereira, Colombia
Email: wjgil@utp.edu.co

C. Orozco-Henao
Programa de Ingeniería Eléctrica
Universidad del Norte
Barranquilla, Colombia
Email: chenaoa@uninorte.edu.co

***Abstract*—This paper presents the development of a nonlinear controller for the reaction wheel pendulum (RWP) via an interconnection and damping assignment passivity-based control (IDA-PBC) approach. The IDA-PBC approach works with the port-Hamiltonian open-loop dynamics of the RWP to propose a nonlinear controller that preserves the Hamiltonian structure in closed-loop by guaranteeing stability properties in the sense of Lyapunov. Numerical results confirm the theoretical development presented throughout simulations in Simulink package from MATLAB. Comparison with a Lyapunov-based approach is also provided.**

***Index Terms*—Energy functions, Lyapunov's stability analysis, reaction wheel pendulum, passivity-based control.**

I. Introduction

Nonlinear dynamic systems are common components at industrial systems [1]. The nonlinear dynamic is even increased in those systems after including control strategies as in the following examples: thermal processes [2], [3], transportation systems [4], [5], electrical machines (motors/generators) [6], [7], power electronic converters [8], [9], pendulums [10], [11], mobile bots [12], among others.

The development of control strategies in these systems could imply difficulties, since it is needed to lead with problems such as parametric uncertainties [13], strong nonlinear functions [14] or the need of measures of all the state variables [15]. In addition, most of the dynamic systems have under-actuate structures [16], which complicate their control design.

Here, we are interested in analyzing the reaction wheel pendulum (RWP) since it is a nonlinear dynamic system typically employed to validate control strategies [13], [16]. Additionally, this system has a similar structure to the classical model of a synchronous machine to make a transient analysis. Therefore, developing efficient control strategies on it can be extrapolated for large-scale and complex systems [9].

The RWP was introduced initially by Spong [10]. This is a variant of the inverted pendulum, which has a bar which can spin freely around the support point (pivot) at one of its end, as is depicted in Fig. 1. Note that the RWP has a motor coupled to the opposite end of the pivot, acting on a wheel of inertia to control φ through the reaction torque τ. The angle φ of the pendulum (from the vertical) and the angle α between the

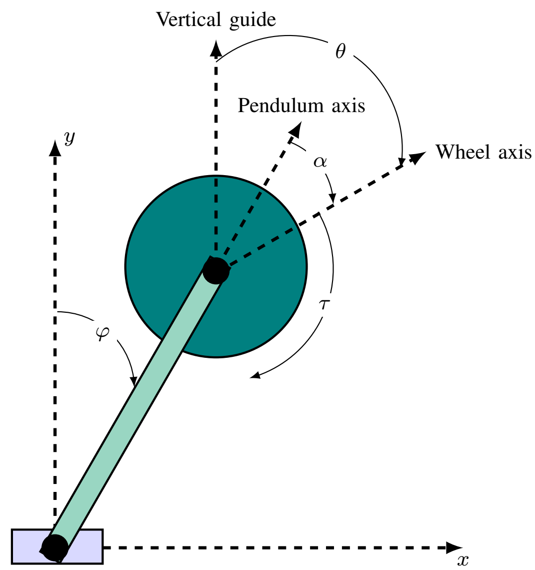

Fig. 1. Representative scheme of the RWP

pendulum and the wheel are measured with sensors located on each of the axes of rotation [15].

The analysis of the RWP can be concentrated in two different objectives. Firstly, the possibility of controlling the pendulum in the inverted position (upright) [16]. Secondly, it is to develop swinging-up strategies to carry-out the pendulum from its rest position to the inverted position [13]. For the first objective, it has been proposed in specialized literature control strategies such as artificial neural networks [14], fuzzy logic [17], trajectory tracking [18], and regulation energy strategies [19], [20]. In the second objective, control approaches such as fuzzy logic [21], extended-feedback linearization [16], [14], Lyapunov-based control approach [13], sliding control [22], exact feedback linearization [10], [18] and passivity-based control based on a Lagrangian formulation [1], have proposed in specialized literature.

In the literature there are absence of works about passivity controlling this system; therefore, we proposed an interconnection and damping passivity-based control (IDA-

PBC) to maintain the pendulum to the upright position. For this purpose, a port-Hamiltonian analysis is presented, which allows preserving passivity properties during the closed-loop operation by designing a nonlinear control law based on energy storage functions (Lyapunov-like analysis). The theoretical development, as well as the simulation results, confirm the efficiency and effectiveness of the proposed IDA-PBC approach even if it is compared with a Lyapunov-based approach.

This paper is organized as follows: Section II presents the nonlinear dynamic formulation of the RWP system as well as the main assumption for reducing the order of the model. Section III presents the general theory related to the IDA-PBC approach. In Section IV, the control design based on IDA-PBC method is presented by highlighting the advantage of using the open-loop Hamiltonian function for generating the closed-loop one. Section V shows the numerical results that validate the proposed control approach in comparison with a nonlinear controller based on Lyapunov functions. Finally, Section VI shows the concluding remarks of this paper as well as the possible future works.

II. Dynamic model of the RWP

The development of the dynamic model of the RWP is based on the schematic representation presented in Fig. 1. If we employ Lagrangian or Newtonian formulations, the following dynamic model of the RWP is attained,

Defining $\theta = \varphi + \alpha$, the dynamical model of the RWP system can be written as follows:

$$\begin{aligned} \ddot{\varphi} &= a \sin(\varphi) - bu, \\ \ddot{\theta} &= cu, \end{aligned} \tag{1}$$

where a, b and c are constants related to the physical parameters of the system, φ represents the angular position of the pendulum measured from the vertical axis, and θ is the relative angle of the reaction wheel measured from the same vertical reference.

To transform the set of equations (1) to a state-space representation, the following state variables are defined: $x_1 = \varphi$, $x_2 = \dot{x_1}$ and $x_3 = \dot{\theta}$. After substituting these into (1), one obtains

$$\begin{aligned} \dot{x}_1 &= x_2, \\ \dot{x}_2 &= a \sin(x_1) - bu, \\ \dot{x}_3 &= cu. \end{aligned} \tag{2}$$

Assumption 1. *The dynamics of the angular speed variable depend exclusively on the control input structure, which implies that its behavior is stable if and only if the control input is bounded and well defined. Based on this, the third term of (2) will be completely solved as follows*

$$x_3 = c \int_{t_0}^{t} u(z)\, dz. \tag{3}$$

Based on the Assumption 1, the dynamic system (2) is reduced to

$$\begin{aligned} \dot{x}_1 &= x_2, \\ \dot{x}_2 &= a \sin(x_1) - bu, \end{aligned} \tag{4}$$

Power systems literature refers to this equation as the swing equation [23].

Lemma 1. *Dynamic system (4) can be represented as a port-Hamiltonian structure as follows*

$$\dot{x} = \mathcal{J} \nabla \mathcal{H}(x) + gu, \tag{5}$$

where $\mathcal{J}$ is a skew-symmetric matrix known as the interconnection matrix, i.e., $\mathcal{J} - \mathcal{J}^T = 0$; $\mathcal{H}(x)$ is the Hamiltonian function, typically named as energy storage function[1]*; g is the control input vector.*

Proof. The dynamic system (4) can be rewritten as (5) by comparing both systems, which produces

$$\begin{gathered} \begin{pmatrix} \dot{x}_1 \\ \dot{x}_2 \end{pmatrix} = \begin{bmatrix} 0 & 1 \\ -1 & 0 \end{bmatrix} \begin{pmatrix} \mathcal{H}_{x_1} \\ \mathcal{H}_{x_2} \end{pmatrix} + \begin{pmatrix} 0 \\ b \end{pmatrix} u \\ \mathcal{H}_{x_i} = \tfrac{\partial}{\partial x_i} \mathcal{H}(x_1, x_2) \end{gathered} \tag{6}$$

in addition, as recommended in [13], the Hamiltonian function of the system can ba calculated as the algebraic sums of the potential and kinetic energies of the pendulum, which can be written as

$$\mathcal{H}(x_1, x_2) = 2a\cos^2\left(\frac{1}{2}x_1\right) + \frac{1}{2}x_2^2. \tag{7}$$

which completes the proof. □

A. Equilibrium points

To determine the possible equilibrium points of the RWP, we can recur the location of the maximums or minimums of the Hamiltonian function. In addition, to know it, the equilibrium points are stable or unstable, the Jacobian criterion can be used.

Note that if we applied the gradient operator on $\mathcal{H}(x_1, x_2)$ to obtain the equilibrium points, then, the following equality must be hold

$$\begin{pmatrix} \mathcal{H}_{x_1} \\ \mathcal{H}_{x_2} \end{pmatrix} = \begin{pmatrix} -a \sin(x_1) \\ x_2 \end{pmatrix} = \begin{pmatrix} 0 \\ 0 \end{pmatrix} \tag{8}$$

which corresponds exactly to the same equilibrium points of (4). Now, by solving (8), the following equilibrium points are reached

$$\begin{aligned} x_1^\star &= n\pi \\ x_2^\star &= 0 \end{aligned} \tag{9}$$

where $n \in \mathbb{Z}$. For representing in better way the vertical up position or vertical down positions, the number n can be split for pair and impair numbers as follows: pair numbers $n = 2k$, impair numbers $n = 2k + 1$, with $k \in \mathbb{Z}$. This substitution produce two possible equilibrium points, i.e., $\mathbf{p}_1(2k\pi, 0)$ and $\mathbf{p}_2((2k + 1)\pi, 0)$.

[1]Note that ∇ is the gradient operator.

B. Nature of the equilibrium points

To determine the nature of the equilibrium points $\mathbf{p}_1$ and $\mathbf{p}_2$, the Jacobian matrix is employed in conjunction with the eigenvalues criteria. Let us calculate the Jacobian matrix from (8) as follows

$$\nabla^2\mathcal{H}(x) = \begin{bmatrix} -a\cos(x_1) & 0 \\ 0 & 1 \end{bmatrix} \tag{10}$$

due to (10) is a diagonal matrix, then, the eigenvalues corresponds to each diagonal value, which implies that

$$\begin{gathered} \lambda_1 = -a\cos(x_1) \\ \lambda_2 = 1 \end{gathered} \tag{11}$$

Definition 1. *If the function $\mathcal{H}(x_1, x_2)$ has a critical point in **p**, and $\nabla^2\mathcal{H}(x_1, x_2)$ is its Jacobian matrix, then **p** can be classified by using the eigenvalues of $\mathcal{J}(x_1, x_2)$ as follows:*

1. *If $\nabla^2\mathcal{H}(x_1, x_2)$ is positive definite, that is, $\lambda_1 > 0$ and $\lambda_2 > 0$ with $\lambda_1, \lambda_2 \in \mathbb{R}$, then **p** is a local minimum.*
2. *If $\nabla^2\mathcal{H}(x_1, x_2)$ is positive definite, that is, $\lambda_1 < 0$ and $\lambda_2 < 0$ with $\lambda_1, \lambda_2 \in \mathbb{R}$, then **p** is a local maximum.*
3. *If $\nabla^2\mathcal{H}(x_1, x_2)$ is neither positive nor negative definite, that is, if either $\lambda_1 > 0$ and $\lambda_2 < 0$ or $\lambda_1 < 0$ and $\lambda_2 > 0$ with $\lambda_1, \lambda_2 \in \mathbb{R}$, then **p** is a saddle point.*
4. *If $\nabla^2\mathcal{H}(x_1, x_2)$ has complex eigenvalues, then this criterion is indecisive.*

When Definition 1 is applied over $\mathbf{p}_1$ and $\mathbf{p}_2$, the following conclusions are reached

$$\begin{gathered} \mathbf{p}_1 \rightarrow \left.\begin{matrix} x_1 = 2k\pi \\ x_2 = 0 \end{matrix}\right\} \; k \in \mathbb{Z} \quad \text{saddle point} \rightarrow \text{unstable} \\ \mathbf{p}_2 \rightarrow \left.\begin{matrix} x_1 = (2k+1)\pi \\ x_2 = 0 \end{matrix}\right\} \; k \in \mathbb{Z} \quad \text{local min.} \rightarrow \text{stable} \end{gathered} \tag{12}$$

Remark 1. *The main objective of controlling a reaction wheel pendulum is held the vertical up position, i.e., the focus of control is becoming $\boldsymbol{p}_1$ into a stable equilibrium point with some bounded and well defines control input u.*

III. IDA-PBC approach

The passivity-based control approach works with the open-loop Hamiltonian model of the dynamic system under analysis (see Eq. (6)) for proposing a closed-loop structure that guarantees stability in the sense of Lyapunov.

Definition 2. *Consider that for the dynamic system () there is a control input u such that it can be transformed into*

$$\dot{x} = [\mathcal{J}_d - \mathcal{R}_d]\,\nabla\mathcal{H}_d(x), \tag{13}$$

where $\mathcal{J}_d$ and $\mathcal{R}_d$ are the skew-symmetric and damping matrices, which implies that $\mathcal{J}_d = -\mathcal{J}_d^T$ and $\mathcal{R}_d \succ 0$ (positive definite); $\mathcal{H}_d(x)$ is the Hamiltonian function under closed-loop operation.

Lemma 2. *If the Hamiltonian function $\mathcal{H}_d(x)$ fulfills the first two Lyapunov conditions, i.e., $\mathcal{H}_d(0) = 0$ and $\mathcal{H}_d(x) > 0\ \forall x \neq 0$; then, the dynamical model (13) is asymptotically stable in the sense of Lyapunov.*

Proof. Suppose that $\mathcal{H}_d(x)$ fulfills the first two Lyapunov conditions; then, if we take is temporal derivative, the following result is reached

$$\dot{\mathcal{H}}_d(x) = \nabla\mathcal{H}_d(x)^T\dot{x}, \tag{14}$$

now, if we substitute the dynamic system (13) into (14), then, the following result is achieved

$$\dot{\mathcal{H}}_d(x) = \nabla\mathcal{H}_d(x)^T[\mathcal{J}_d - \mathcal{R}_d]\,\nabla\mathcal{H}_d(x). \tag{15}$$

If we take the advantage that the desired interconnection matrix is skew-symmetric, then, the expression (15) is reduced to

$$\dot{\mathcal{H}}_d(x) = -\nabla\mathcal{H}_d(x)^T\mathcal{R}_d\nabla\mathcal{H}_d(x) > 0, \tag{16}$$

which is clearly a quadratic form, implying that it is negative definite if and only if the damping matrix is positive definite, and the proof is complete, since the second condition of the Lyapunov's theorem is guaranteed by the IDA-PBC approach. □

Remark 2. *All the analysis presented in this paper take focus on the origin of coordinates since $\boldsymbol{p}_1$ is the equilibrium point under interest, which is achieved when $k = 0$ as can be seen in (12).*

IV. Control design

To obtain a general control input that allows transforming the open-loop dynamics (6) into the close-loop structure (13), let us assume that the desired Hamiltonian function is

$$\mathcal{H}_d(x) = \mathcal{H}(x) + h(x_1), \tag{17}$$

where $h(x_1)$ is the energy storage component added for guaranteeing that $\mathcal{H}_d(x)$ fulfills the first two Lyapunov's theorem conditions.

To guarantee that $\mathbf{p}_1$ is an stable equilibrium point, let us obtain from (17) the Jacobian matrix, which produces

$$\nabla^2\mathcal{H}_d(x) = \begin{bmatrix} -a\cos(x_1) + \frac{d^2}{dx_1^2}h(x_1) & 0 \\ 0 & 1 \end{bmatrix} \tag{18}$$

which implies by following Definition 1 that $\mathbf{p}_1$ be stable if and only if $\lambda_1 > 0$; which implies that the next constraint must be satisfied

$$-a\cos(x_1) + \frac{d^2}{dx_1^2}h(x_1) > 0. \tag{19}$$

To solve the constraint (19), we assume that the following equality must be hold with $\alpha_1 > 0$

$$\frac{d^2}{dx_1^2}h(x_1) = \alpha_1 + a\cos(x_1). \tag{20}$$

Note that the solution of (20) can be easily achieved using ordinary differential equation methods as reported in [24]. A possible (feasible) solution of (20) is presented below

$$h(x_1) = \frac{1}{2}\alpha_1 x_1^2 - a\cos(x_1) + \alpha_2 x_1 + \alpha_3. \tag{21}$$

where α_2 and α_3 are real constants.

With the solution reported in (21), the desired Hamiltonian function (17), takes the following form

$$\mathcal{H}_d(x) = \left(\begin{array}{l} 2a\cos^2\left(\frac{1}{2}x_1\right) + \frac{1}{2}x_2^2 + \\ \frac{1}{2}\alpha_1 x_1^2 - a\cos(x_1) + \alpha_2 x_1 + \alpha_3 \end{array} \right), \quad (22)$$

now, to fulfill that $\mathcal{H}_d(x)$ is equal to zero when $x = 0$, let us select $\alpha_2 = 0$ and $\alpha_3 = a$. In addition, to proof that $\mathcal{H}_d(x) > 0$, $\forall x \neq 0$, let us to recur to the following classical trigonometric property

$$\cos\left(\frac{1}{2}x_1\right) = \pm\sqrt{\frac{1+\cos(x_1)}{2}}, \quad (23)$$

If we substitute (23) into (22), then the desired closed-loop Hamiltonian function takes the following form

$$\mathcal{H}_d(x) = \frac{1}{2}x_2^2 + \frac{1}{2}\alpha_1 x_1^2, \quad (24)$$

which clearly shows that $\mathcal{H}_d(x)$ is a positive definite Lyapunov function, and the stability of $\mathbf{p}_1$ is guaranteed.

To select the control input, let us also define the desired interconnection and damping matrices as

$$\mathcal{J}_d - \mathcal{R}_d = \begin{bmatrix} r_1 & j_1 \\ -j_1 & r_2 \end{bmatrix} \quad (25)$$

Note that, the closed-loop dynamics (13) can be represented by using (24) and (25) as follows

$$\begin{pmatrix} \dot{x}_1 \\ \dot{x}_2 \end{pmatrix} = \begin{bmatrix} r_1 & j_1 \\ -j_1 & r_2 \end{bmatrix} \begin{pmatrix} \alpha_1 x_1 \\ x_2 \end{pmatrix} \quad (26)$$

now, by equaling the open-loop dynamics (6) with the closed-loop dynamics (26), the following control law is obtained

$$u = \frac{1}{b}\left(a\sin(x_1) - j_1\alpha_1 x_1 + r_2 x_2\right) \quad (27)$$

Remark 3. *To guarantee the same numerical convergence reported in [13] for a Lyapunov controller, we select here* $r_1 = 0$, $j_1 = -1$, $\alpha_1 = 3500$ *and* $r_2 = 135$, *which are the values that we will use in the simulation section.*

Remark 4. *Due to* r_1 *is equal to zero, it is necessary to recur to the Barbalat's lemma for proving that* $\boldsymbol{p}_1$ *is asymptotically stable as can be consulted in [24].*

V. Numerical results

The numerical validation of the proposed approach is carry-out by MATLAB software with its Ordinary Differential Equation (ODE45) package. The parameters of the RWP system are presented in Table I. In addition, the initial conditions for all tasks are $x_1 = 0.12$ rad and $x_2 = 0$ rad/s, and also the limits of the control signal are assumed to be between -10 and 10.

As comparative approach, we employ a recent developed nonlinear controller based on Lyapunov functions recently proposed in [13]; the resultant control law is as follow

$$u = \frac{1}{b}\left(k_1 x_1 + k_2 x_2 + 2a\sin(x_1)\right), \quad (28)$$

where $k_1 = 3500$ and $k_2 = 135$ as feedback gains.

TABLE I
RWP Parameters [15]

a	b	c
78.4 $\left(\frac{rad}{s}\right)^2$	1.08 $\frac{rad}{s^2}$	198 $\frac{rad}{s^2}$

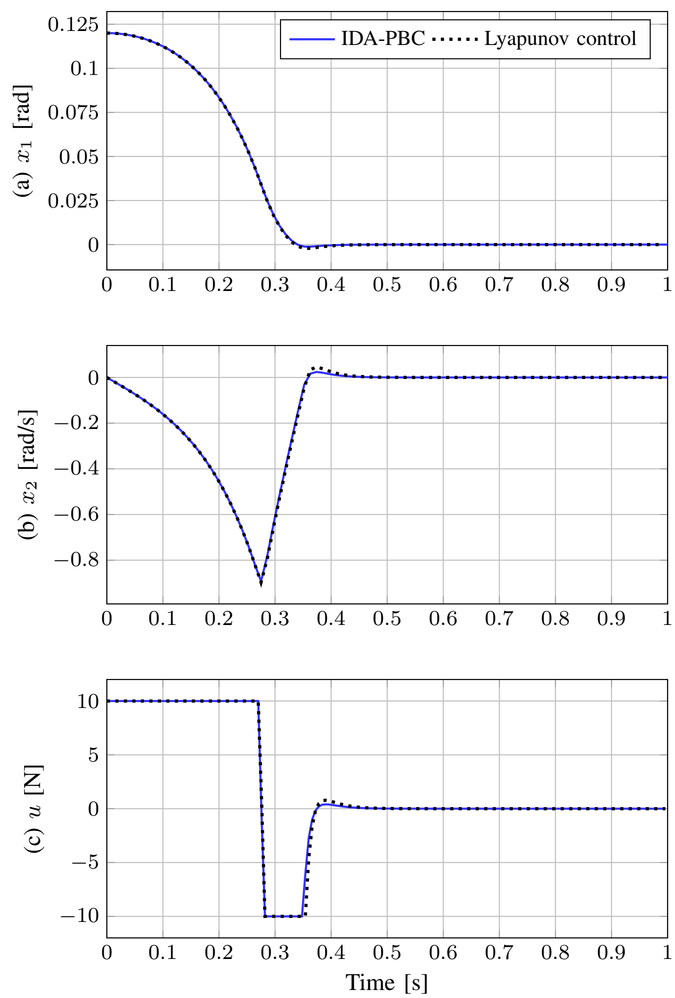

Fig. 2. Dynamical performance of the proposed and comparative control approaches without uncertainties: (a) angular position of the pendulum, (b) angular speed of the pendulum, and (c) control input

A. Operation under ideal conditions

In this scenario, we consider that all the parameters of the pendulum are perfectly known, i.e., without uncertainties. Fig. 2 shows the comparison between the proposed IDA-PBC approach and the Lyapunov-based controller.

Note that both controllers reach the control objective after 0.4 s as can be seen in Fig 2(a), with minimal overpass (0.0012 for IDA-PBC and 0.0023 for Lyapunov-based control), by responding as quasi first order dynamical system. On the other hand, Fig. 2(b) shows the dynamical performance of the angular speed of the pendulum, which achieves the zero value at the same time that the angular position reaches the vertical up position. For controlling the RWP from the initial position to the equilibrium point $\mathbf{p}_1$ the control input has some zones undersaturation (from 0 s to 0.36 s), due to the physical constraint imposed in this input (see Fig. 2(c)); notwithstanding, this numerical simulation shows that the stability performance of the RWP system is not compromised under these conditions.

B. Operation under model uncertainties

A parametric uncertainty in the RWP model can be expressed by rewritten (6) as follows [25], [26],

$$\begin{pmatrix} \dot{x}_1 \\ \dot{x}_2 \end{pmatrix} = \begin{pmatrix} x_2 \\ a\sin(x_1) \end{pmatrix} + \Delta \begin{pmatrix} x_1 \\ x_2 \end{pmatrix} + \begin{pmatrix} 0 \\ -b \end{pmatrix} u$$

with Δ being the parametric uncertainty with all the elements equal to 1.5 as recommended in [13].

Fig. 3 shows the dynamical performance of the state variables and control input when IDA-PBC and Lyapunov-based control approaches are tested under parametric uncertainties; note that the angular position of the pendulum experiences in both cases a second-order dynamic behavior by reaching the control goal when time is 0.5 s (see Fig. 3(a)). In addition, the maximum overpass of the IDA-PBC is 0.0403 rad (about $2.3075°$), while the Lyapunov-based controller has an overpass about 0.0420 rad ($2.4052°$), which implies that our proposed IDA-PBC method has minor overpass (about $0.1°$), being efficient in comparison to the Lyapunov-based method.

Fig. 3(b) shows that the uncertainties imply that the angular speed of the pendulum has higher efforts in comparison to the first case, since the control input (see Fig. 3(c)) with uncertainties has three periods of saturation against two when uncertainties were inexistent. Finally, it is important to mention as that under this scenario of operation the RWP experiences a stable performance independently of the saturation conditions of the control input, which is an advantage considering the strong nonlinearities of the RWP system.

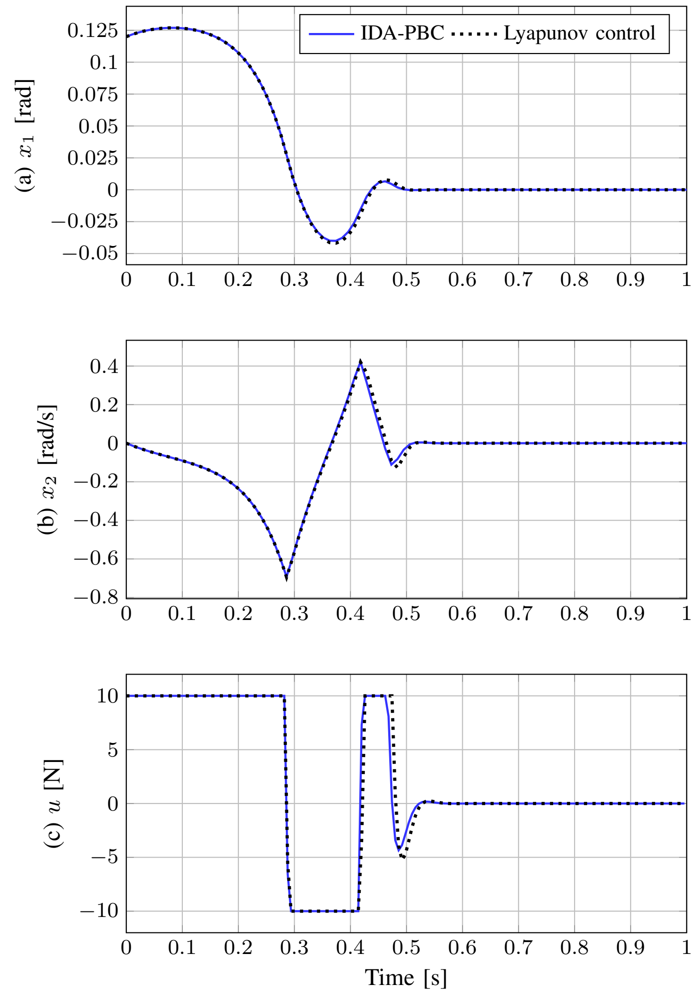

Fig. 3. Dynamical performance of the proposed and comparative control approaches with uncertainties:: (a) angular position of the pendulum, (b) angular speed of the pendulum, and (c) control input

VI. Conclusions and Future Works

The Hamiltonian open-loop representation of the RWP was derived in this paper, and it was used for proposing a passivity-based controller by injecting damping and interconnection actions through the IDA-PBC approach. The proposed IDA-PBC approach allows guaranteeing stability operation in closed-loop by modifying the energy storage function for becoming the vertical up position as the global minimum. A Lyapunov-based approach was provided to compare the effectiveness of the proposed IDA-PBC approach under ideal and non-ideal conditions (i.e., with uncertainties in the model), which show that the IDA-PBC approach has small overpasses in the angular position of the RWP in contrast to the Lyapunov-based method where the overpasses were higher. Simulations results allowed to demonstrate that the stability of the system was not be compromised by the saturation of the control input since the sign of the saturation is governed by the behavior of this control input, which implies that it only will affect the time of response to achieve the control objective.

As future work, it will be possible to replace the proposed controller by an artificial neural network that allows making a global control strategy including the swing-up of the pendulum and its stabilization in the vertical up position. In addition, experimental validation of the proposed approach, as well as Lyapunov-based methods, will help to understand the advantages of nonlinear controller designs over classical linear approximations. Also, this work could be extended to power systems using similar structure, then extended to multi-machine power systems

Financial Support

This work was partially supported in part by the National Scholarship Program Doctorates of the Administrative Department of Science, Technology and Innovation of Colombia (COLCIENCIAS), by calling contest 727-2015, and in part by Universidad Tecnológica de Bolívar, under Projects C2018P020 and C2019P011.

References

[1] M. Ryalat and D. S. Laila, "A simplified IDA-PBC design for underactuated mechanical systems with applications," *European Journal of Control*, vol. 27, no. Supplement C, pp. 1 – 16, 2016.

[2] U.-C. Moon, Y. Lee, and K. Y. Lee, "Practical dynamic matrix control for thermal power plant coordinated control," *Control Eng. Pract.*, vol. 71, pp. 154 – 163, 2018.

[3] M. M. Shajahan, D. N. Jamal, V. Aparna, and M. A. Khan, "Control of electric power generation of thermal power plant in TamilNadu," *Case Studies in Thermal Engineering*, vol. 12, pp. 728 – 735, 2018.

[4] R. Wai and J. Lee, "Adaptive Fuzzy-Neural-Network Control for Maglev Transportation System," *IEEE Trans. Neural Netw.*, vol. 19, no. 1, pp. 54–70, Jan 2008.

[5] X. Liang, Y. Fang, N. Sun, and H. Lin, "Nonlinear Hierarchical Control for Unmanned Quadrotor Transportation Systems," *IEEE Trans. Ind. Electron.*, vol. 65, no. 4, pp. 3395–3405, April 2018.

[6] W. Gil-González, A. Garces, and A. Escobar, "Passivity-based control and stability analysis for hydro-turbine governing systems," *Appl. Math. Modell.*, vol. 68, pp. 471 – 486, 2019. [Online]. Available: http://www.sciencedirect.com/science/article/pii/S0307904X18305870

[7] R. Salim, A. Mansouri, A. Bendiabdellah, S. Chekroun, and M. Touam, "Sensorless passivity based control for induction motor via an adaptive observer," *ISA Transactions*, vol. 84, pp. 118 – 127, 2019. [Online]. Available: http://www.sciencedirect.com/science/article/pii/S0019057818303719

[8] D. D. Murdock and D. G. Taylor, "Balancing a reaction wheel pendulum with PM synchronous motor actuation," in *IECON 2014 - 40th Annual Conference of the IEEE Industrial Electronics Society*, Oct 2014, pp. 96–102.

[9] W. Gil-González, O. D. Montoya, and A. Garces, "Direct power control for VSC-HVDC systems: An application of the global tracking passivity-based PI approach," *Int. J. Electr. Power Energy Syst.*, vol. 110, pp. 588 – 597, 2019. [Online]. Available: http://www.sciencedirect.com/science/article/pii/S0142061518333519

[10] M. W. Spong, P. Corke, and R. Lozano, "Nonlinear control of the Reaction Wheel Pendulum," *Automatica*, vol. 37, no. 11, pp. 1845 – 1851, 2001.

[11] S. Irfan, A. Mehmood, M. T. Razzaq, and J. Iqbal, "Advanced sliding mode control techniques for Inverted Pendulum: Modelling and simulation," *Engineering Science and Technology, an International Journal*, vol. 21, no. 4, pp. 753 – 759, 2018.

[12] B. Hichri, J.-C. Fauroux, L. Adouane, I. Doroftei, and Y. Mezouar, "Design of cooperative mobile robots for co-manipulation and transportation tasks," *Rob. Comput. Integr. Manuf.*, vol. 57, pp. 412 – 421, 2019.

[13] O. D. Montoya and W. Gil-González, "Nonlinear analysis and control of a reaction wheel pendulum: Lyapunov-based approach," *Engineering Science and Technology, an International Journal*, 2019.

[14] O. D. Montoya, C. A. Ramírez, and L. F. Grisales, "Global Control of Reaction Wheel Pendulum Using Artificial Neural Networks and Extended Linearization," *Scientia et technica*, vol. 22, no. 20, pp. 130–140, jun 2017.

[15] D. J. Block, K. J. Åström, and M. W. Spong, "The reaction wheel pendulum," *Synthesis Lectures on Control and mechatronics*, vol. 1, no. 1, pp. 1–105, 2007.

[16] O. D. Montoya, L. F. Grisales-Noreña, V. D. Correa-Ramírez, and D. Giraldo-Buitrago, "Global control of reaction wheel pendulum through energy regulation and extended linearization of the state variables," *Tecno Lógicas*, vol. 17, no. 32, pp. 33–46, Jun. 2014.

[17] K. Srinivas and L. Behera, "Swing-up control strategies for a reaction wheel pendulum," *Int. J. Syst. Sci.*, vol. 39, no. 12, pp. 1165–1177, 2008.

[18] V. D. Correa-Ramírez, D. Giraldo-Buitrago, and A. Escobar-Mejía, "Fuzzy control of an inverted pendulum Driven by a reaction wheel using a trajectory tracking scheme," *Tecno Lógicas*, vol. 20, no. 39, pp. 1–13, Aug. 2017.

[19] B. Bapiraju, K. N. Srinivas, P. P. Kumar, and L. Behera, "On balancing control strategies for a reaction wheel pendulum," in *Proceedings of the IEEE INDICON 2004. First India Annual Conference, 2004.*, Dec 2004, pp. 199–204.

[20] I. Fantoni, R. Lozano, and M. W. Spong, "Stabilization of the reaction wheel pendulum using an energy approach," in *2001 European Control Conference (ECC)*, Sep. 2001, pp. 2552–2557.

[21] J. G. Valenzuela, O. D. Montoya, and D. Giraldo-Buitrago, "Local control of reaction wheel pendulum using fuzzy logic," *Scientia et Technica*, vol. 18, no. 4, pp. 623–632, Dec. 2013.

[22] D. Gutiérrez-Oribio, A. Mercado-Uribe, J. A. Moreno, and L. Fridman, "Stabilization of the Reaction Wheel Pendulum via a Third Order Discontinuous Integral Sliding Mode Algorithm," in *2018 15th International Workshop on Variable Structure Systems (VSS)*, July 2018, pp. 132–137.

[23] P. Kundur, *Power System Stability and Control*, MCGRAW-HILL, Ed. McGraw-Hill Education - Europe, 2005.

[24] L. Perko, *Differential Equations and Dynamical Systems*, ser. Texts in Applied Mathematics. Springer New York, 2013.

[25] K.-J. Lin, "Stabilization of uncertain fuzzy control systems via a new descriptor system approach," *Computers & Mathematics with Applications*, vol. 64, no. 5, pp. 1170–1178, 2012.

[26] A. M. El-Nagar, M. El-Bardini, and N. M. EL-Rabaie, "Intelligent control for nonlinear inverted pendulum based on interval type-2 fuzzy PD controller," *Alexandria Engineering Journal*, vol. 53, no. 1, pp. 23–32, 2014.